

Two-Electron Sensitization: A New Concept for Silver Halide Photography

Ian R. Gould,^{*,†} Jerome R. Lenhard,* Annabel A. Muentner, Stephen A. Godleski, and Samir Farid*

Contribution from the Research Laboratories, Eastman Kodak Company, Rochester, New York 14650, and the Department of Chemistry and Biochemistry, Arizona State University, Tempe, Arizona 85287

Received June 23, 2000. Revised Manuscript Received September 27, 2000

Abstract: The primary process in conventional photography involves electron transfer from an excited dye molecule into the conduction band of a silver halide microcrystal. Repeated events of this type ultimately lead to formation of a small, stable cluster of silver atoms in the silver halide that acts as the latent image, along with the one-electron oxidized forms of the dye molecules. Here we describe a new concept for increasing the efficiency of photographic systems, two-electron sensitization, which makes use of the chemical potential stored in the oxidized dyes. In conventional photography, subsequent reactions of the oxidized dyes are not controlled and may in fact include counterproductive return electron transfer reactions (recombination). In the two-electron sensitization scheme, an appropriately designed electron donor molecule, X–Y, that is added to the photographic dispersion transfers an electron to the oxidized dye to give a radical cation, X–Y^{•+}. The X–Y^{•+} then undergoes a fragmentation reaction to give a radical, X[•], and a stable cation, Y⁺. The radical X[•] is chosen to be sufficiently reducing so that it can inject an electron into the silver halide conduction band. In this way, the oxidized dye, which is a *strong oxidant*, is replaced by the radical, X[•], which is a *strong reductant*. The two-electron transfer scheme has the potential of doubling the photographic speed because two electrons are injected per absorbed photon. Here we describe the mechanistic details of the two-electron sensitization scheme and the structural and energetic criteria for the X–Y molecules. Several electron-rich carboxylate molecules that meet these criteria have been identified. Solution-phase experiments to determine the fragmentation (decarboxylation) kinetics and the reducing power of the resultant radicals are described. Photographic data demonstrate that increases in sensitivity by factors approaching 2 can be obtained, confirming the viability of the two-electron sensitization concept.

Introduction

One of the major challenges in the development of technologies that use or convert light energy is to maximize their photoefficiency. In applications involving photoinduced electron transfer reactions, minimizing the energy-wasting return electron transfer is often a primary goal in this regard.¹ For image capture and information storage, amplification of the primary photoinduced electron transfer event is also usually required.² Silver halide photography offers by far the highest sensitivity to light of all applications that use photoinduced electron transfer, primarily owing to the inherent sensitivity to light of the silver halide system and to the high amplification achieved during the development process.³

Conventional photographic systems are based on silver halide microcrystals dispersed in gelatin.³ Silver halide materials are semiconductors with band gap absorptions that depend on the exact halide composition but generally absorb strongly only below ~450 nm.⁴ Sensitivity beyond the band gap absorption region is achieved through organic dyes adsorbed onto the

surface of the crystals.^{5,6} Upon photoexcitation, the dye transfers an electron to the silver halide conduction band, eq 1.⁵ This electron is subsequently trapped in the form of a single silver atom, a species that is unstable with respect to return electron transfer (recombination) to the oxidized dye. However, with more light absorption events, multiple photoelectrons can be injected, and a small, stable cluster of metallic silver can form, Ag_n⁰, eq 2.⁵ This small cluster of silver atoms, which constitutes a latent image, can catalyze reduction of the entire silver halide crystal by a suitable reducing reagent in the development process.⁷ Usually, only four silver atoms are required to form a latent image that can be developed.^{5,7} For some practical silver halide systems, as few as 10 absorbed photons per crystal are actually required to form the latent image,⁸ which subsequently catalyzes the reduction of the approximately 10¹⁰ silver ions in the microcrystal. This is the origin of the enormous amplification

(4) Moser, F.; Ahrenkiel, R. K. In *The Theory of the Photographic Process*, 4th ed.; James, T. H., Ed.; MacMillan: New York, 1977; p 37.

(5) West, W.; Gilman, P. B. In *The Theory of the Photographic Process*, 4th ed.; James, T. H., Ed.; MacMillan: New York, 1977; p 251.

(6) (a) Usually, the adsorbed dyes are at fairly high coverage and are aggregated in the form of a "J-aggregate".^{6b} (b) Herz, A. H. *Adv. Colloid Interface Sci.* **1977**, *8*, 237.

(7) Fyson, J. R.; Twist, P. J.; Gould, I. R. In *Electron Transfer in Chemistry, Vol. 5, Molecular-level Electronics, Imaging and Information, Energy and the Environment*; Balzani, V., Ed.; Wiley-VCH: New York, in press.

(8) Tani, T. In *Photographic Sensitivity*; Oxford University Press: Oxford, 1995; pp 235–237.

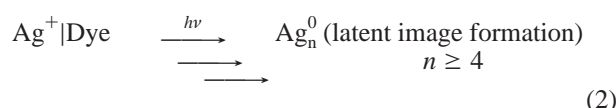
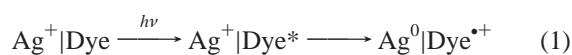
[†] Department of Chemistry and Biochemistry, Arizona State University.

(1) (a) Gould, I. R.; Farid, S. *Acc. Chem. Res.* **1996**, *29*, 522. (b) Graetzel, M.; Moser, J. E. In *Electron Transfer in Chemistry, Vol. 5, Molecular-level Electronics, Imaging and Information, Energy and the Environment*; Balzani, V., Ed.; Wiley-VCH: New York, in press.

(2) Jacobson, K. I.; Jacobson, R. E. In *Imaging Systems*; Wiley: New York, 1976.

(3) *The Theory of the Photographic Process*, 4th ed.; James, T. H., Ed.; MacMillan: New York, 1977.

which is characteristic of silver halide photography.⁹

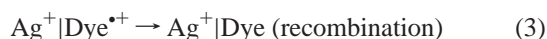


Despite the high efficacy of silver halide as an imaging sensor, there is a continuing demand for photographic materials with still higher photoefficiency. The majority of past efforts along these lines have been directed toward improving photoefficiency through chemical modifications of the silver halide crystal, which are designed to modulate photoelectron trapping in ways that minimize recombination. Examples of such modifications include alteration of the composition and location of the halide,¹⁰ the introduction of sulfur-containing surface sites,¹¹ and the inclusion of dopant ions into the crystal lattice.¹² In contrast, relatively little attention has been paid to improving photoefficiency by altering the chemistry associated with the oxidized spectral sensitizing dye.

Here we describe a novel concept for photosensitization of silver halide dispersions that takes this latter approach. This concept, which we call two-electron sensitization, provides a means to prevent electron-hole recombination and, because two electrons are injected per absorbed photon, has the potential for doubling the photosensitivity of silver halide dispersions. The mechanism is based on a secondary electron transfer reaction with the photooxidized sensitizing dye, and follow-up radical ion chemistry. The first part of this report describes the concept and the associated energetic and structural requirements for the secondary electron donor. In the second part, tests of the concept and the chemistry of secondary donor molecules in model solution-phase systems are described. In the third part, the application of the concept to photographic systems is briefly described.

Concept

As shown in eq 1, the product of photoinduced electron transfer from an excited dye to the silver halide crystal is a dye radical cation. Prior to the formation of a stable latent image, return electron transfer from the conduction band to this dye radical cation might take place, eq 3. This energy-wasting, recombination reaction results in lower overall photoefficiency. The first goal of the present approach is to minimize such recombination.¹³



Thus, the first step in the proposed mechanism is an exothermic secondary electron transfer reaction from a donor

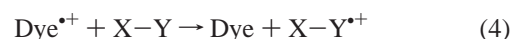
(9) (a) In addition to electron-hole recombination, other loss processes that limit the practical quantum sensitivity of silver halide include dispersity (the formation of more than one latent image cluster per crystal), regression (the destruction of latent image clusters by reaction with mobile holes), and the formation of internal latent image that is inaccessible to the developer solution.^{9b} (b) Hamilton, J. F. In *The Theory of the Photographic Process*, 4th ed.; James, T. H., Ed.; MacMillan: New York, 1977; pp 105–128.

(10) (a) Tani, T. In *Photographic Sensitivity*; Oxford University Press: Oxford, 1995; pp 24–41. (b) Bando, S.; Shibahara, Y.; Ishimaru, S. *J. Imaging Sci.* **1985**, 29, 193. (c) Maskasky, J. E. *Photogr. Sci. Eng.* **1981**, 25, 96.

(11) (a) Hamilton, J. F. *Adv. Phys.* **1988**, 37, 359. (b) Harbison, J. M.; Spencer, H. E. In *The Theory of the Photographic Process*, 4th ed.; James, T. H., Ed.; MacMillan: New York, 1977; p 152.

(12) (a) Eachus, R. S.; Olm, M. T. *Annu. Rep. Prog. Chem., Sect. C: Phys. Chem.* **1986**, 83, 3. (b) Eachus, R. S.; Olm, M. T. *Cryst. Lattice Defects Amorphous Mater.* **1989**, 18, 297. (c) Belloni, J.; Treguer, M.; Remita, H.; deKeyser, R. *Nature* **1999**, 402, 865.

molecule, X–Y, which is located at or near the silver halide crystal, to the dye radical cation, eq 4.¹⁴ Reduction of the oxidized dye



according to eq 4 will result in physical separation of the conduction band electron and the oxidized dye, thus reducing the rate of recombination and perhaps increasing the quantum efficiency. In addition to minimizing recombination, however, a further goal of the present approach is to use the *chemical potential* stored in the dye radical cation to do useful work. Unlike applications such as solar energy conversion^{1b} or electrophotography,^{13b} where it is important that no net chemical reaction results from the photoinduced electron transfer so that the redox cycle can be repeated many times, irreversible chemical reactions can be used in silver halide photography. The second step in our scheme then is to use an electron donor that undergoes a fragmentation reaction upon being oxidized to the radical cation (X–Y^{*+}). The products of this fragmentation are a radical (X^{*}) and a cation (Y⁺), eq 5.



Although the secondary electron transfer reaction of eq 4 should slow recombination based on physical separation of the charges, the reaction products X^{*} and Y⁺ can be chosen so that return electron transfer of a conduction band electron is highly endothermic, essentially eliminating this process.

The final step in the proposed scheme is the most crucial one. If the radical X^{*} resulting from the radical cation fragmentation is chosen to be a strong reducing agent, it can undergo another electron transfer reaction with the silver halide, eq 6, thus injecting a *second electron* into the conduction band.

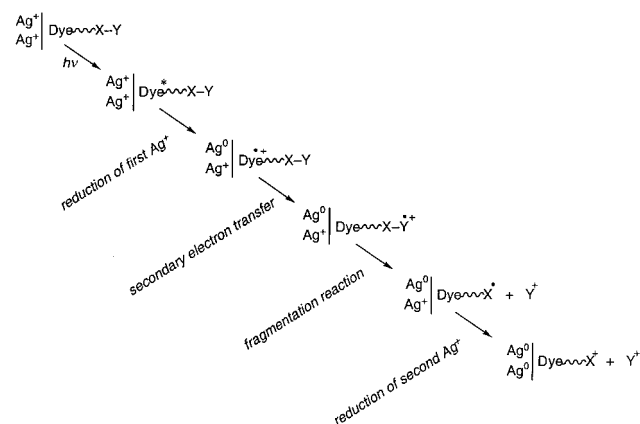


The overall process is illustrated schematically in Scheme 1. Formally, the light energy is used to inject the two electrons that constitute the covalent bond between the X and Y moieties into the conduction band of silver halide. The two-electron injection process uses the chemical potential of the oxidized dye (which is usually wasted) and is driven by the formation of two stable cations, X⁺ and Y⁺. The transfer of two electrons per photon has the potential for doubling the photographic sensitivity of a dye-sensitized silver halide system. Under ideal circumstances, the combination of the two-electron injection process and the irreversible trapping of the dye radical cation to reduce possible recombination may result in a speed increase by even more than a factor of 2.

(13) (a) As discussed in the Introduction, minimizing recombination is a major concern in all systems that are based on photoinduced electron transfer. In several systems, this recombination has been essentially eliminated. For example, charge separation occurs with close to unit efficiency in electrophotographic applications.^{13b} In this case, charge separation is made energetically more favorable by an applied electric field.^{13b} (b) Weiss, D. S.; Cowdery, J. R.; Young, R. H. In *Electron Transfer in Chemistry, Vol. 5, Molecular-level Electronics, Imaging and Information, Energy and the Environment*; Balzani, V., Ed.; Wiley-VCH: New York, in press.

(14) This is entirely analogous to the well-known photosynthetic reaction center system, where exothermic secondary electron transfer occurs from the primary electron acceptor to a critically positioned secondary acceptor resulting in charge separation with essentially unit efficiency.^{14b} A similar approach has also been described in recent work on sensitization of titanium dioxide for solar energy conversion applications.^{14c} (b) Woodbury, N. W.; Allen, J. P. In *Anoxygenic Photosynthetic Bacteria*; Blankenship, R. E., Madigan, M. T., Bauer, C. E., Eds.; Kluwer: Boston, 1995; Chapter 24. (c) Bonhote, P.; Moser, J.-E.; Humphry-Baker, R.; Vlachopoulos, N.; Zakeeruddin, S. M.; Walder, L.; Graetzel, M. *J. Am. Chem. Soc.* **1999**, 121, 1324.

Scheme 1



A similar scheme would also apply to silver halide systems that do not contain the sensitizing dye. In this case, band gap absorption of light by the silver halide gives a conduction band electron and a valence band hole. Electron transfer from the X–Y molecule to the hole in the valence band would initiate the same series of reactions as those outlined above for the dye-sensitized systems.

Although the proposed scheme for sensitization of silver halide is novel, several of the individual processes are well-known. For example, the use of fast fragmentation reactions to compete with return electron transfer has been described several times.¹⁵ Examples of multielectron photoprocesses have also been reported, both for homogeneous and heterogeneous redox systems. For example, Whitten et al. have described one-photon/two-electron photoreduction reactions in systems containing the electron donor triethylamine.¹⁶ After an initial one-electron transfer from the amine to a photoexcited acceptor, the amine cation radical can deprotonate to form a neutral radical which is a powerful reducing agent and can deliver a second electron to the electron acceptor. A related process wherein highly reducing radicals are formed has also been described for semiconductor photoelectrochemical devices.¹⁷ During band gap irradiation of n-type semiconductors, highly energetic holes can oxidize electron donors present in solution. Neutral radicals can subsequently be formed via a fragmentation process. Morrison has shown that, when sufficiently reducing, these radicals can inject a second electron into the semiconductor material, thereby effecting a doubling of the photoelectric current.¹⁷ On TiO₂, this current doubling process has been observed with a wide variety of species, including alcohols, hydrocarbons, and amines.¹⁷ In addition to these systems, related reactions were also reported in nonphotoinduced processes. For example, Bard used the oxidation of oxalate, which fragments to give a strong reductant, CO₂^{•-}, in electrogenerated chemiluminescence.¹⁸ Examples of analogous chemically induced oxidation followed by fragmentation and formation of a reducing radical are also known.¹⁹

(15) See, for example: (a) Fox, M. A. In *Advances in Photochemistry*; Volman, D. H., Hammond, G. S., Gollnick, K., Eds.; Wiley: New York, 1986; Vol. 13, p 237. (b) Maslak, P. *Top. Curr. Chem.* **1993**, *168*, 1.

(16) (a) Gaillard, E. R.; Whitten, D. G. *Acc. Chem. Res.* **1996**, *29*, 292. (b) Kellett, M. A.; Whitten, D. G.; Gould, I. R.; Bergmark, W. R. *J. Am. Chem. Soc.* **1991**, *113*, 358.

(17) (a) Morrison, S. R.; Freund, T. *J. Phys. Chem.* **1967**, *47*, 1543. (b) Morrison, S. R. In *Electrochemistry of Semiconductor Oxidized Metal Electrodes*; Plenum Press: New York, 1980; p 219. (c) Forouzan, F.; Richards, T. C.; Bard, A. J. *J. Phys. Chem.*, **1996**, *100*, 18123. (d) Schoenmakers, G. H.; Vanmaekelgergh, D.; Kelly, J. J. *J. Chem. Soc., Faraday Trans.* **1997**, *93*, 1127.

(18) (a) Chang, M.-M.; Saji, T.; Bard, A. J. *J. Am. Chem. Soc.* **1977**, *99*, 5399. (b) Rubinstein, I.; Bard, A. J. *J. Am. Chem. Soc.* **1981**, *103*, 512. (c) Kanoufi, F.; Bard, A. J. *J. Phys. Chem. B* **1999**, *103*, 10469.

Energetic, Kinetic, and Structural Requirements. For successful implementation of the two-electron mechanism, the three reactions involving the X–Y molecule should be energetically and kinetically feasible. These are trapping of the dye^{•+}, fragmentation of X–Y^{•+} to form X[•], and electron injection into the silver halide conduction band by X[•].

Dye^{•+} trapping (eq 4) is energetically favorable if the oxidation potential of the X–Y molecule is comparable to, or is less positive than that of the sensitizing dye. Common blue-, green-, and red-absorbing silver halide sensitizing dyes (usually cyanines) typically have oxidation potentials around 1.4, 1.2, and 0.9 V vs SCE, respectively.²⁰ Accordingly, the range of potential X–Y donor molecules will be wider for use with blue-sensitizing dyes simply because these dyes have higher oxidation potentials. The oxidation potential of the X–Y donor has a practical lower limit, however. This is because very low oxidation potential donors can be sensitive to aerial oxidation and are generally less thermally stable. In addition, donors with very low oxidation potentials may reduce silver halide in a thermal reaction, resulting in nonimaging formation of a latent image. Given these considerations, the oxidation potential for X–Y should preferably be ~0.1–0.5 V less positive than that of the associated sensitizing dye.

To be useful, fragmentation of the X–Y^{•+} should occur faster than other undesirable reactions, such as return electron transfer to X–Y^{•+} from the silver halide conduction band, or nucleophilic addition to X–Y^{•+} or other possible chemical reactions. The required rates for fragmentation of X–Y^{•+} are thus not easily defined, because the rates of these competing processes are not well-known. For example, electron recombination may occur over a wide range of time scales, perhaps from subpicoseconds to seconds in the heterogeneous silver halide/gelatin dispersions.²¹ In the mainly aqueous environment of gelatin, it is likely that nucleophilic attack will occur on a millisecond time scale.²² This implies that the rate constants for X–Y^{•+} fragmentation should at least be greater than 10³ s⁻¹ and that even faster fragmentation may be required to compete effectively with electron recombination.

For exothermic electron injection from X[•], eq 6, the oxidation potential of X[•] should be more negative than the potential required to inject an electron into the conduction band of silver halide. An estimate of this potential can be obtained from the limiting reduction potential of dyes that photosensitize silver halide or that quench (desensitize) latent image formation of directly excited silver halide. For silver bromide cubes at pAg of 8, this limiting reduction potential is ~-0.9 V.^{20a,23} Although this value is expected to vary slightly with changes in silver halide composition, we conclude that the oxidation potential of X[•] should be approximately -0.9 V, or more negative.

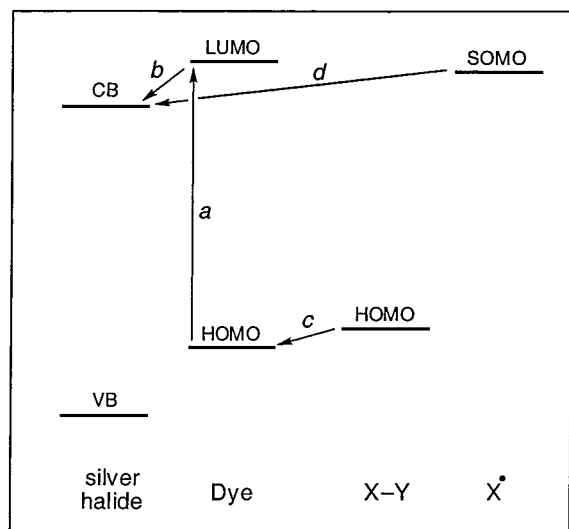
(19) (a) Fukuzumi, S.; Kitano, T.; Ishikawa, M. *J. Am. Chem. Soc.* **1990**, *112*, 5631. (b) Kochi, J. K. *Organometallic Mechanism and Catalysis*; Academic Press: New York, 1978.

(20) (a) Lenhard, J. *J. Imaging Sci.* **1986**, *30*, 27. (b) Lenhard, J. R.; Hein, B. R.; Muentner, A. A. *J. Phys. Chem.* **1993**, *97*, 8269. (c) Gilman, P. B. *Photogr. Sci. Eng.* **1974**, *18*, 475.

(21) (a) Tani, T. *Photographic Sensitivity*; Oxford University Press: Oxford, 1995; pp 143–148. (b) Hamilton, J. F. *Adv. Phys.* **1988**, *37*, 359.

(22) See, for example: Mattes, S. L.; Farid, S. In *Organic Photochemistry*; Padwa, A., Ed.; Marcel Dekker: New York, 1983; Vol. 6, p 233. (b) Davidson, R. S. In *Advances in Physical Organic Chemistry*; Gold, V., Bethell, D., Eds.; Academic Press: London, 1983; Vol. 19, p 130. (c) *Photoinduced Electron Transfer Reactions, Part C. Photoinduced Electron Transfer Reactions: Organic Substrates*; Fox, M. A.; Chanon, M., Eds.; Elsevier: Amsterdam, 1988. (d) Mattay, J. *Synthesis*, **1989**, 233.

(23) (a) Loutfy, R. O.; Sharp, J. H. *Photogr. Sci. Eng.* **1976**, *20*, 165. (b) Eachus, R. S.; Marchetti, A. P.; Muentner, A. A. *Annu. Rev. Phys. Chem.* **1999**, *50*, 117.

Scheme 2^a

^a Key: (a) Photoexcitation of the sensitizing dye. (b) Electron transfer from the excited dye to the conduction band. (c) Electron transfer from the fragmentable electron donor X-Y to the oxidized dye. This requires the HOMO of X-Y to be higher than the HOMO of the dye. (d) Electron transfer from the fragmentation product X• to the conduction band. This requires the singly occupied molecular orbital, SOMO, of X• to be higher than the conduction band of silver halide, but not necessarily higher than the LUMO of the sensitizing dye.

The energetics of the electron transfer processes are determined by the relative positions of the relevant molecular orbitals of the dye, X-Y, and the radical X• together with the conduction and valence bands of the silver halide, as illustrated in Scheme 2.

Of these thermodynamic and kinetic requirements, the reducing power of the radical X• is the most difficult to meet. Oxidation potentials of numerous free radicals have been measured by transient electrochemical and pulse radiolysis techniques.^{24,25} Of the radicals that have been studied to date, those with heteroatoms in the α positions are found to be the easiest to oxidize. Specifically, α -amino radicals have oxidation potentials in the necessary range of ~ -0.9 V.²⁴ This observation suggested that amines are likely candidates for X-Y.

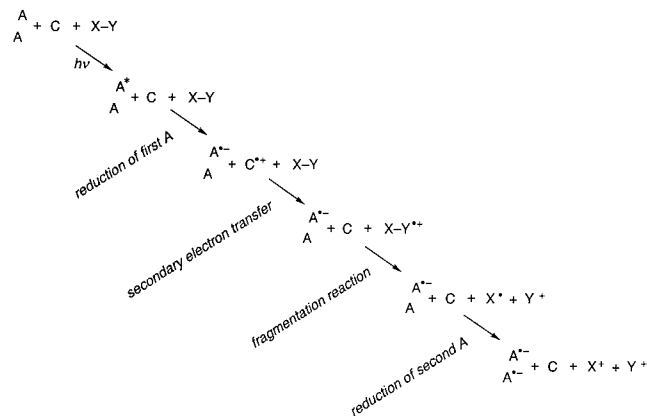
A number of known fragmentation reactions for X-Y⁺ can be considered,^{15,16,22,26} including decarboxylation,^{26a-c} desilylation,^{26d} C-C bond cleavage,^{15b,16} and deprotonation,^{26e-h} and a number of these reactions have been studied for the case of amines.²⁷ Of these, decarboxylation initially seemed to be the most useful, both because these reactions appeared to be fairly efficient for amine radical cations²⁷ and because of the ready access to carboxyl-substituted amines. The only potential problem with amines is that they should not be protonated under the aqueous conditions of silver halide photography. This final requirement precludes the use of simple aliphatic amines, for

(24) (a) Wayner, D. D.; McPhee, D. J.; Griller, D. *J. Am. Chem. Soc.* **1988**, *110*, 132. (b) Griller, D.; Wayner, D. D. *M. Pure Appl. Chem.* **1989**, *61*, 717.

(25) (a) Rao, P. S.; Hayon, E. *J. Am. Chem. Soc.* **1974**, *96*, 1287. (b) Rao, P. S.; Hayon, E. *J. Am. Chem. Soc.* **1975**, *97*, 2985. (c) Rao, P. S.; Hayon, E. *J. Phys. Chem.* **1975**, *79*, 397.

(26) (a) Budac, D.; Wan, P. *J. Photochem. Photobiol., A* **1992**, *67*, 135. (b) Steenken, S.; Warren, C. J.; Gilbert, B. C. *J. Chem. Soc., Perkin Trans. 2* **1990**, 335. (c) Davidson, R. S.; Steiner, P. R. *J. Chem. Soc., Perkin Trans. 2* **1972**, 1557. (d) Dockery, K. P.; Dinnocenzo, J. P.; Farid, S.; Goodman, J. L.; Gould, I. R.; Todd, W. P. *J. Am. Chem. Soc.* **1997**, *119*, 1876. (e) Lewis, F. D. *Acc. Chem. Res.* **1986**, *19*, 401. (f) Schlesener, C. J.; Amatore, C.; Kochi, J. K. *J. Am. Chem. Soc.* **1984**, *106*, 7472. (g) Dinnocenzo, J. P.; Banach, T. E. *J. Am. Chem. Soc.* **1989**, *111*, 8646. (h) Parker, V. D.; Tilset, M. *J. Am. Chem. Soc.* **1991**, *113*, 8778.

Scheme 3



which the protonated forms have pK_a 's in the range of ~ 9.5 – 10.5 ,²⁸ because the normal pH of photographic dispersions is ~ 5.5 .²⁹

Solution-Phase Studies

Experimental Approach. Transient absorption experiments were used to investigate a series of X-Y molecules in model studies in solution. By using transient absorption spectroscopy, oxidation potentials of the intermediate radicals X• can be obtained using an “energy bracketing” approach.²⁵ Although obviously not as accurate as the electrochemical method,²⁴ the oxidation potentials determined this way are accurate enough for the present purposes. More importantly, the transient absorption approach also provides valuable kinetic information.

Electron transfer to the excited acceptor 9,10-dicyanoanthracene (DCA, A in Scheme 3) from the high oxidation potential cosensitizer biphenyl (C in Scheme 3) was used to form the separated radical ions, A^{•-} and C^{•+}, with high efficiency.³⁰ In the presence of $\sim 10^{-3}$ M X-Y, which has a lower oxidation potential than C, secondary electron transfer occurs to generate free X-Y^{•+}, also in high yield and within 100 ns of the excitation laser pulse. The reactions were carried out in a 4:1 acetonitrile/water mixture, which approximates the somewhat aqueous environment of a silver halide/gelatin photographic dispersion. Importantly, the reduction potential of DCA of -0.91 V vs SCE is very close to the value of ~ -0.9 V, which has been estimated for the conduction band reduction potential in silver halide, as mentioned above. Thus, X• radicals that can reduce DCA to DCA^{•-} should presumably also inject electrons into the conduction band of the silver halide crystal. Thus, Scheme 3 is closely related to the two-electron sensitization scheme for silver halide. The acceptor A takes the place of the silver halide, C takes the place of the dye, and the X-Y donor plays the same role in each process. The DCA is excited and the initial photoinduced electron transfer from C forms one DCA^{•-}. This is followed by secondary electron transfer from X-Y to the radical cation, C^{•+}, to generate the radical cation, X-Y^{•+}, which fragments to give a radical, X•, that might reduce

(27) (a) Su, Z.; Mariano, P. S.; Falvey, D. E.; Yoon, U. C.; Oh, S. W. *J. Am. Chem. Soc.* **1998**, *120*, 10676. (b) Su, Z.; Falvey, D. E.; Yoon, U. C.; Mariano, P. S. *J. Am. Chem. Soc.* **1997**, *119*, 5261. (c) Yoon, U. C.; Mariano, P. S.; Givens, R. S.; Atwater, B. W. *Adv. Electron Transfer Chem.* **1994**, *4*, 117. (d) Zhang, X.; Yeh, S.-R.; Hong, S.; Freccero, M.; Albini, A.; Falvey, D. E.; Mariano, P. S. *J. Am. Chem. Soc.* **1994**, *116*, 4211.

(28) Kortum, G.; Vogel, W.; Andrussov, K. In *Dissociation Constants of Organic Acids in Aqueous Solution*; Butterworth: London, 1961.

(29) Rose, P. I. In *The Theory of the Photographic Process*, 4th ed.; James, T. H., Ed.; MacMillan: New York, 1977; p 51.

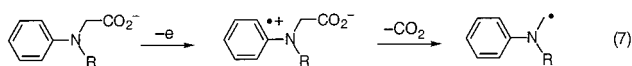
(30) Gould, I. R.; Ege, D.; Moser, J. E.; Farid, S. *J. Am. Chem. Soc.* **1990**, *112*, 4290.

a second DCA molecule. The $\text{DCA}^{\bullet-}$ has a characteristic absorption maximum at 705 nm, which can be used to follow the overall reaction mechanism and kinetics.³⁰ Thus, the DCA system represents a very useful tool for evaluating donors in homogeneous solution as potential donor species in the two-electron sensitization scheme. If reduction of two DCA molecules per photon can be observed as a consequence of the reaction sequence for $X-Y$ in solution, injection of two electrons into the conduction band per absorbed photon will presumably occur if $X-Y$ can be incorporated in the silver halide sensitization sequence.

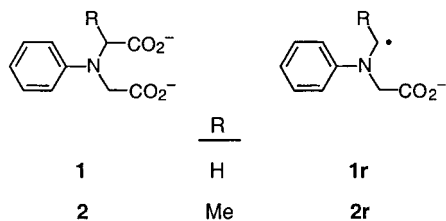
When sufficiently exothermic, the rate of reaction between the radical X^{\bullet} and DCA to give the second $\text{DCA}^{\bullet-}$ should be close to the diffusion-controlled limit. At the DCA concentrations used in the experiments ($1-1.5 \times 10^{-4}$ M), this reaction should thus occur with a time constant of $\sim 1 \mu\text{s}$. If the radical cation $X-Y^{\bullet+}$ fragmentation is much faster than this and electron transfer from X^{\bullet} to DCA is exothermic, then the transient absorption signal should show "immediate" formation of the first $\text{DCA}^{\bullet-}$, followed by a slower grow-in of the second $\text{DCA}^{\bullet-}$ on a time scale of $\sim 1 \mu\text{s}$. Ideally, the intensity of the signal due to the slowly formed second $\text{DCA}^{\bullet-}$ will be equal to that due to the first. Absence of grow-in of $\text{DCA}^{\bullet-}$ may be due to unfavorable energetics for reduction of DCA by the radical X^{\bullet} or because fragmentation of the $X-Y^{\bullet+}$ is too slow to compete with bimolecular return electron transfer with $\text{DCA}^{\bullet-}$.

If the oxidation potential of X^{\bullet} is not sufficiently negative to reduce DCA, an estimate of its reducing power can be obtained by using other cyanoanthracenes as acceptors in an "energy bracketing" approach. We have also used 2,9,10-tricyanoanthracene, TriCA, and 2,6,9,10-tetracyanoanthracene, TCA, which are easier to reduce by nearly one-fourth and by nearly one-half of a volt, respectively, Scheme 4.^{30,31}

Amine Decarboxylation. Previous measurements indicated that α -amino radicals have oxidation potentials that are among the most negative of those that have been studied.²⁴ Thus, we explored the reactivity of molecules, which upon oxidative decarboxylation, eq 7, give radicals that are α - to an aromatic amine.²⁷ The general amine structure shown in eq 7 is an



example of an *N*-phenyl-substituted amino acid. The kinetics of decarboxylation of the radical cations of such species have been studied previously by Mariano.²⁷ For practical applications, thermal stability is of crucial importance, and in our hands, bis-carboxylates such as compounds **1** and **2** were found to be more stable than the monocarboxylates.



We were also interested in exploring the scope of useful reactions that would yield strongly reducing radicals, beyond that described in the literature. For example, it was not clear whether appropriately substituted vinylogue and benzylogue amino radicals would be strong enough reducing agents to be

(31) The reduction potential of TriCA was measured under the same conditions as those used for DCA and TCA.³⁰

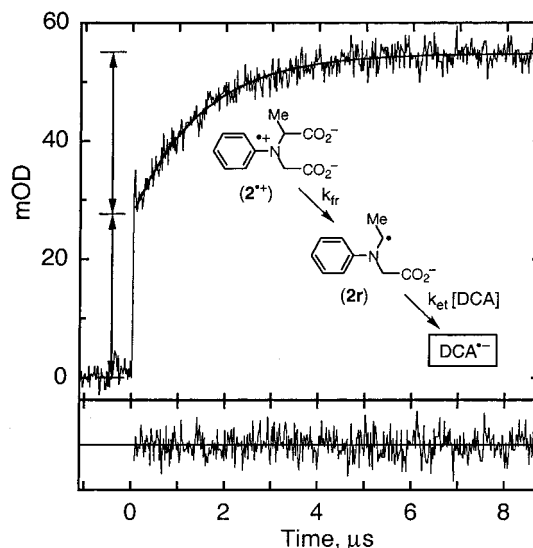
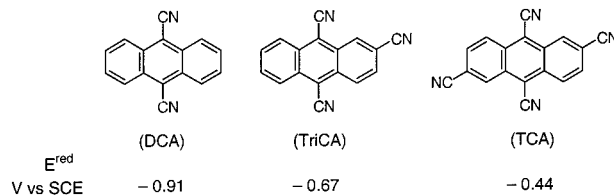


Figure 1. Optical density (in units of 10^{-3} , mOD) at 705 nm, as a function of time, t , observed upon excitation (410 nm) of an argon-purged 1:4 water/acetonitrile solution of DCA ($\sim 1.5 \times 10^{-4}$ M), biphenyl (0.12 M), and compound **2** (2×10^{-3} M). The absorbance at this wavelength is due to $\text{DCA}^{\bullet-}$. The initial, very rapid formation of $\text{DCA}^{\bullet-}$ is indicated by the jump in optical density at $t = 0$. The subsequent rise in optical density is due to fragmentation of the radical cation $2^{\bullet+}$ to give the radical $2r^{\bullet}$ that reduces a second molecule of DCA. In this case the fragmentation reaction is much faster than the bimolecular rate of reduction of DCA by $2r^{\bullet}$. Consequently, the grow-in approximates pseudo-first-order kinetics fairly accurately. The smooth curve represents the best fit to the data and is given by: $54.83 - 27.54 \exp(-6.9 \times 10^5 t)$.

Scheme 4



useful in a two-electron silver halide sensitization scheme. It was also of interest to find out whether substrates other than aromatic amines could produce sufficiently reducing radicals.

Structural Dependence of Radical Reducing Power. As indicated above, time-resolved experiments were used to study the reducing power of the X^{\bullet} . Pulsed laser excitation of a DCA/biphenyl solution in the presence of **2** clearly shows delayed formation of a second $\text{DCA}^{\bullet-}$, Figure 1. The rate constant for grow-in of the second $\text{DCA}^{\bullet-}$ ($\sim 7 \times 10^5 \text{ s}^{-1}$ at 1.5×10^{-4} M DCA concentration) is consistent with close to diffusion-controlled reduction of DCA by the radical $2r^{\bullet}$. Thus, the oxidation potential of $2r^{\bullet}$ must be more negative than the reduction potential of DCA, -0.91 V, and the fragmentation of the radical cation of **2** must be considerably faster than the observed rate of reduction of the second DCA by $2r^{\bullet}$ (see further below). Similar behavior is observed in the reaction of **1** using TriCA as the acceptor. Thus, the oxidation potential for **1r** must be more negative than the reduction potential of TriCA, -0.67 V.

For **1**, with DCA as the acceptor, grow-in of $\text{DCA}^{\bullet-}$ is also observed. In this case, however, the signal due to the second $\text{DCA}^{\bullet-}$ is smaller than that of the first, and the grow-in rate is smaller than those for **2** with DCA or TriCA. The size and the grow-in rate are also sensitive to the energy of the excitation

Table 1^a

Compound	(E ^{ox}) _{X•} ^a (V vs SCE)	(k _{fr}) _{X-V^{•+}} ^b (s ⁻¹)	λ _{obs} ^c (nm)
1	-0.86 ± 0.03	1.8 × 10 ⁷	550
2	-0.96 ± 0.03	>1 × 10 ⁸	--- ^d

3	>-0.4	2.3 × 10 ⁷	580
4	-0.56 ± 0.08	6.5 × 10 ⁷	
5	-0.79 ± 0.08	2.1 × 10 ⁸	
6	<-0.9	>3 × 10 ⁸	--- ^d

7	>-0.4	4.3 × 10 ⁴	470 - 510
8	<-0.9	5 × 10 ⁵	
9	<-0.9	6.7 × 10 ⁵	
10	<-0.9	2.6 × 10 ⁷	470

^a Estimated oxidation potential of the corresponding radical formed upon oxidative decarboxylation, in V vs SCE. See text for error estimates in each case. ^b Rate constant for decarboxylation of the corresponding radical cation, measured in acetonitrile with 20% water. See text for details. The experimental error is estimated to be ~15% in each case. ^c Observation wavelength for time-resolved absorption measurements of radical cation decarboxylation rate constant. ^d Radical cation too short-lived to be directly detected.

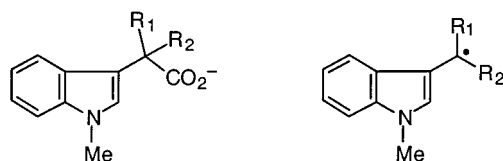
laser pulse. At [DCA] of 1.4 × 10⁻⁴ M, the grow-in rate extrapolated to zero laser energy is ~2 × 10⁵ s⁻¹ (compared to 7 × 10⁵ s⁻¹ for **2** with DCA), and the extrapolated "yield" of the second DCA radical anion is ~60%. The yield of the second DCA^{•-} increases with temperature, and at 60 °C nearly complete two-electron transfer is observed, although the grow-in rate remains slower than the corresponding rate for the **2r**/DCA system (3.6 × 10⁵ vs 1.3 × 10⁶ s⁻¹). These observations suggest less favorable energetics for reduction of DCA by the radical **1r**. Electrochemical measurements indicate that the oxidation potentials of primary α-amino radicals such as **1r** are ~0.1 V more positive than those for the corresponding secondary radicals such as **2r**.²⁴ Thus, the different behavior of **1r** and **2r** in their reactions with DCA can be explained if the oxidation potentials of these radicals bracket the reduction potential of DCA. It is, therefore, reasonable to assign oxidation potentials of ~-0.86 V and of ~-0.96 V for **1r** and **2r**, respectively.

Decarboxylation of *N*-methylindole acetic acid, **3**, via photo-induced electron transfer has been described previously.³² The product radical, **3r**, is a vinylogue α-amino radical that has been used as an efficient initiating system for radical polymerization.³² Transient absorption experiments using **3** do not lead to two-electron reduction even with TCA as the acceptor, indicating that the oxidation potential of **3r** is less negative than -0.4 V. The vinylogous radicals are evidently harder to oxidize than the α-amino radicals **1r** and **2r** by at least one-half of a volt.

An increase in the radical reducing power was achieved by increasing the substitution at the radical center as in **4** and **5**.

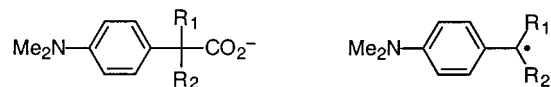
Experiments, as before, with **4** resulted in reduction of two molecules of TCA but not of TriCA. With **5**, reduction of two molecules of TriCA but not of DCA was observed. From these observations we determine that the oxidation potential of **4r** is more negative than -0.44 V and less negative than -0.67 V and that of **5r** is more negative than -0.67 V and less negative than -0.91 V. The diffusion-controlled reduction of a second acceptor molecule indicates that this process is exothermic by at least a few 10 mV. The lack of reduction of a second acceptor molecule indicates endothermicity of a few 10 mV. Thus the oxidation potentials of the radicals **4r** and **5r** are estimated to be ~-0.56 ± 0.08 and ~-0.79 ± 0.08 V vs SCE, respectively (Table 1).

Although the oxidation potentials of the secondary and tertiary radicals **4r** and **5r** are approximately 0.2 and 0.4 V, respectively, more negative than that of the primary radical, **3r**, they are still not reducing enough to donate an electron to DCA and hence, to silver halide. Only with the hydroxy-substituted compound, **6**, was two-electron reduction observed using DCA as the acceptor. The large decrease in oxidation potential in this case is presumably a consequence of stabilization of the positive charge by the α-oxygen.

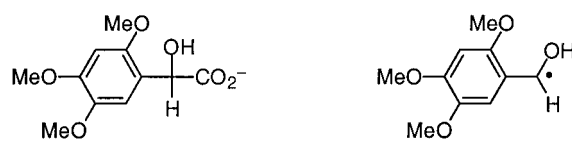


	R ¹	R ²	
3	H	H	3r
4	Me	H	4r
5	Me	Me	5r
6	OH	H	6r

Similar results were obtained for benzylogue derivatives of the α-amino radicals derived from **7–9** as summarized in Table 1. Finally, a radical in which the donating substituents were alkoxy groups instead of an amino group was studied, **10r**, and was found to have an oxidation potential more negative than -0.9 V (Table 1).



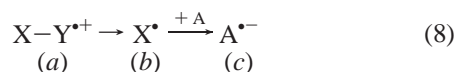
	R ¹	R ²	
7	H	H	7r
8	OH	H	8r
9	OH	Me	9r

**10****10r**

(32) (a) Ledwith, A. In *The Exciplex*; Gordon, M., Ware, W. R., Eds.; Academic Press: New York, 1975; p 209. (b) Williams, J. L. R.; Specht, D. P.; Farid, S. *Polym. Eng. Sci.* **1983**, 23, 1023. (c) Specht, D. P.; Payne, K. L.; Farid, S. Y. U.S. Patent 4,278,751, 1981.

Kinetics of Decarboxylation. As mentioned above, observation of a second reduced acceptor molecule indicates both that

the radical has a more negative oxidation potential than the reduction potential of the acceptor and that fragmentation of the radical cation occurs. The grow-in of the second reduced acceptor follows kinetics described by a consecutive $a \rightarrow b \rightarrow c$ process, where a represents $X-Y^{+\bullet}$, b is X^{\bullet} , and c is $A^{\bullet-}$, eq 8.³³ If the fragmentation process, $a \rightarrow b$, is much faster than reduction of the acceptor by the radical, $b \rightarrow c$, then the grow-in kinetics can be approximated by a single-exponential function, corresponding to the second (slower) process. Thus, whenever the grow-in is observed to occur with a rate of $\sim 10^6$ s⁻¹ at acceptor concentrations of $\sim 10^{-4}$ M and is approximately single exponential, then the radical cation fragmentation rate constant must be considerably larger than 10^6 s⁻¹.



The time-resolved grow-in of the second radical anions with compounds **1–7** and **10** were single exponential, implying fast fragmentation. With **8** and **9**, however, the grow-ins were clearly not single exponential, indicating that fragmentation and reduction were occurring with similar rates. Analysis of the grow-in kinetics for DCA^{•-} according to eq 8 with **9** as the donor gave rates of 6.7×10^5 and 9.1×10^5 s⁻¹, Figure 2b.³³ The second rate is consistent with bimolecular electron transfer from the radical to DCA, as measured for analogous reactions. The former is presumably the fragmentation rate for **9**^{•+}.

The fragmentation kinetics for **9**^{•+} could also be determined by direct observation of the radical cation absorption decay, monitored between 470 and 510 nm. The DCA^{•-} also absorbs in this region, and thus oxygen-saturated solutions are characterized by a sum of two single exponentials: one due to **9**^{•+} decay and one due to reaction of the DCA^{•-} with oxygen, Figure 2a. The rate of the latter reaction was independently determined to be 5.8×10^6 s⁻¹ from the single-exponential decay observed at 705 nm, where DCA^{•-} is the only absorbing species. Fitting the absorption decays at 470–490 nm as a sum of two exponential functions gave rates of 5.7×10^6 and 6.9×10^5 s⁻¹. The former clearly corresponds to decay of the DCA^{•-} and the latter to decay of **9**^{•+}, which we equate with the rate constant for fragmentation. This rate constant of 6.9×10^5 s⁻¹ is very similar to that of 6.7×10^5 s⁻¹, obtained from the grow-in of the second DCA^{•-}, Figure 2b, providing firm support for the assignment of the various transient species.

As mentioned above, fragmentation of the other radical cations was too fast to be determined from the grow-ins of the second acceptor radical anions, and the rate constants for these reactions could be obtained only from observation of the radical cation decay. Experiments were performed under argon or oxygen, depending upon whether the radical anion interfered with the absorption decays. The rates for **1**, **3**, **7**, and **10** were measured at room temperature, and those for **4** and **5** were estimated by extrapolation from measurements at lower temperatures. Those for **2** and **6** were too fast to be measured, and only lower limits could be obtained. The data are summarized in Table 1.

It has been shown that one of the factors that determines the rate constants for bond fragmentation in radical cations is the oxidation potential of the corresponding neutral compound.³⁴ This trend is also observed in the present data. For example, the oxidation potential of **10** is higher by nearly one-third of a

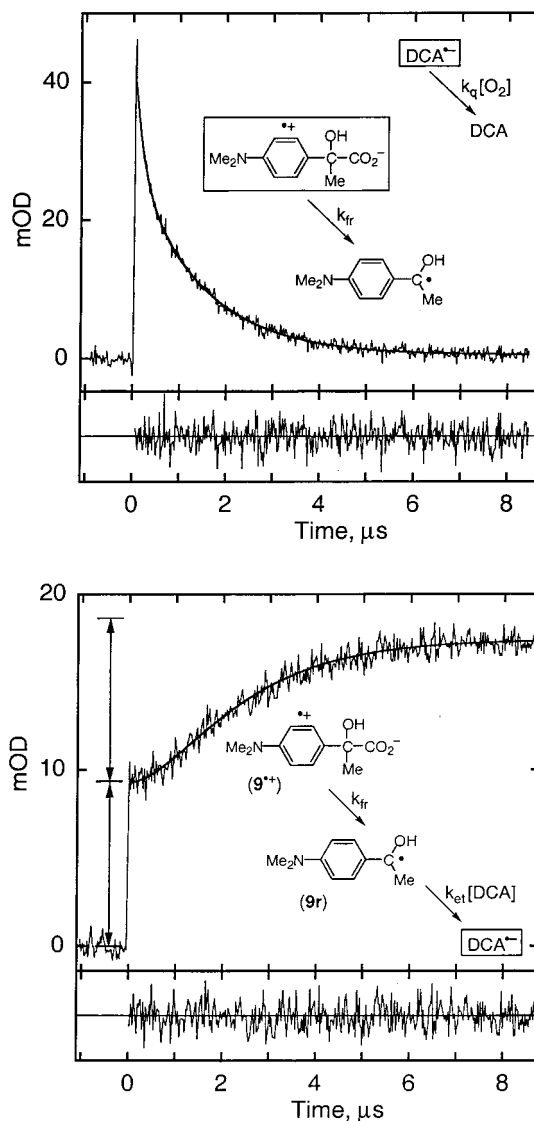


Figure 2. (a, top) Optical density (in units of 10^{-3} , mOD) at 480 nm, as a function of time, t , observed upon excitation (410 nm) of an oxygen-saturated 1:4 water/acetonitrile solution of DCA ($\sim 1.5 \times 10^{-4}$ M), biphenyl (0.12 M), and compound **9** (2×10^{-3} M). Both the radical anion of DCA (DCA^{•-}) and the radical cation **9**^{•+} contribute to the total absorbance, and the decay is thus given by a combination of *two independent first-order components*. The smooth curve represents the best fit to the data and is given by: $19.59 \exp[(-5.7 \times 10^6)t] + 27.89 \exp[(-6.9 \times 10^5)t] + 0.48$. The faster decay corresponds to reaction of DCA^{•-} with oxygen, and the slower decay to fragmentation (decarboxylation) of **9**^{•+}. (b, bottom) Optical density at 705 nm, as a function of time, t , observed upon excitation (410 nm) of the above solution after purging with argon. The absorbance at this wavelength is due only to DCA^{•-}. The initial, very rapid formation of **9**^{•+} and DCA^{•-} is indicated by the jump in optical density at $t = 0$. Subsequently, **9**^{•+} fragments to give the radical, **9r**, that reduces another DCA molecule to form a second DCA^{•-} on a microsecond time scale. The change in absorbance is thus described by a *consecutive a → b → c process in which c is monitored*. The smooth curve represents the best fit to the data taking both processes into account and is given by: $17.42 - 30.58 \exp[(-6.7 \times 10^5)t] + 22.47 \exp[(-9.1 \times 10^5)t]$. The slower component corresponds to the fragmentation of **9**^{•+} ($a \rightarrow b$) and the faster component to the reduction of the second DCA molecule ($b \rightarrow c$).

volt compared to those of **8** and **9**, and the radical cation undergoes much faster fragmentation.³⁵

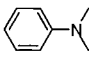
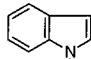
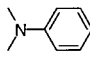
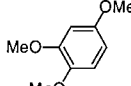
Oxidation Potentials of the Fragmentable Donors, X–Y. The fast fragmentation reactions of the radical cations $X-Y^{+\bullet}$,

(33) Moore, J. W.; Pearson, R. G. In *Kinetics and Mechanism*; Wiley: New York, 1981.

(34) Maslak, P.; Vallombroso, T. M.; Chapman, W. H., Jr.; Narvaez, J. N. *Angew. Chem., Int. Ed. Engl.* **1994**, *33*, 73.

while desirable for the electron-hole separation at the dye/silver halide interface, make an exact experimental determination of the formal oxidation potentials of the X-Y molecules difficult to obtain. Such fast follow-up reactions usually lead to significant shifts in the peak potentials.³⁶ Because only upper limits for the oxidation potentials are required in the present investigation, estimates of the relevant potentials were obtained from measurements of structurally related model compounds. Specifically, compound **11** was used as the model for **1** and **2**, compound **12** for **3-6**, compound **13** for **7-9**, and compound **14** for **10**.

Even some of the model compounds exhibited irreversible oxidation under our electrochemical conditions. As usually observed for anilines, the *p*-substituted **13** showed reversible oxidation at nominal potential scan rates in acetonitrile, whereas **11**, **12**, and **14** showed irreversible oxidation presumably due to radical coupling reactions. A reversible oxidation potential for **11** was thus obtained from a Hammett plot of E^{ox} versus σ^+ , constructed from AC voltammetry data for a series of reversibly oxidized, *p*-substituted dimethylanilines.³⁷ The intercept of this plot, 0.868 V vs SCE, corresponds to the formal oxidation potential, E^{ox} , of the parent dimethylaniline, **11**. The peak potential for the chemically irreversible oxidation of **11** at a scan rate of 0.1 V/s occurs 72 mV less positive than the formal E^{ox} . Accordingly, we estimate the formal E^{ox} for **12** and **14** to be 1.262 and 1.15 V, respectively, by adding 72 mV to the observed peak potentials for these compounds, assuming that the rates of the irreversible chemical reaction for $\mathbf{12}^{\bullet+}$ and $\mathbf{14}^{\bullet+}$ are similar to that of $\mathbf{11}^{\bullet+}$.

				
	11	12	13	14
E^{ox} (V vs SCE)	0.868	1.262	0.732	1.15

On the basis of the data from these model compounds, the estimated oxidation potentials for the fragmentable donors **1-10** indicate that these compounds meet the corresponding energetic requirements identified above.

Summary of Solution-Phase Studies. As discussed above, to be useful in a two-electron sensitization scheme, an X-Y donor must be capable of donating an electron to the oxidized sensitizing dye, must undergo rapid fragmentation, and must provide a radical that can inject an electron into the conduction band of silver halide. The estimated oxidation potentials for all of the donors studied here are close to or lower than those of typical blue- or green-sensitizing dyes ($\geq \sim 1.2$ V vs SCE) and all undergo fragmentation with rate constants greater than 10^4 s⁻¹. Only those compounds which have nitrogen or oxygen atoms in a position adjacent to the radical that results from fragmentation (compounds **1**, **2**, **6**, **8**, **9**, and **10**) have oxidation potentials for the radicals (X^{\bullet}) that are close to or more negative

(35) A detailed kinetic analysis of these and other fragmentable donors, including substituent, temperature, and solvent effects, will be the subject of another publication.

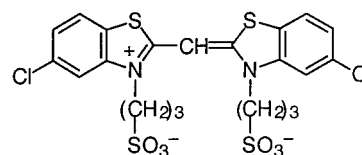
(36) Andrieux, C. P.; Le Gorand, A.; Saveant, J. M. *J. Am. Chem. Soc.* **1992**, *114*, 6892.

(37) (a) This analysis is analogous to that reported by Parker and Tilset.^{37b} The *p*-substituents on *N,N*-dimethylaniline and the Hammett σ^+ values are: MeO (-0.78), Me (-0.31), COOEt (+0.49), and CF₃ (+0.61). The corresponding reversible oxidation potentials that we measured are 0.565, 0.732, 1.06, and 1.117 V vs SCE, respectively. A least-squares fit gives a slope of 0.40 and an intercept of 0.868 V. (b) Parker, V. D.; Tilset, M. J. *Am. Chem. Soc.* **1991**, *113*, 8778.

than ~ -0.9 V vs SCE, the estimated reduction potential of silver halide. Therefore, these compounds are expected to be thermodynamically capable of injecting a second electron into the conduction band of silver halide and thus should provide the highest photographic benefit. The other compounds, which yield less reducing radicals, may still show some photographic advantage due to the fact that they should be capable of trapping the oxidized dyes and thus may decrease the electron-hole recombination probability. These compounds should also serve as useful controls, since they should not inject two electrons.

Photographic Studies

The ability of the fragmentable electron donors **1-10** to enhance the photosensitivity of silver halide was examined using photographic film coatings of a silver iodobromide microcrystalline dispersion that were prepared in aqueous gelatin.^{38,39} Two separate silver iodobromide dispersions were studied, one containing a spectral sensitizing dye and the other with no added dye. The sensitizing dye was a blue-absorbing anionic cyanine dye, **15**, $E^{\text{ox}} = 1.35$ V vs SCE, that exhibits a strong affinity for the silver halide surface and readily forms the familiar *J*-aggregate when adsorbed at near monolayer coverage.^{6b}



15

The film dispersions that contained the sensitizer were given a filtered, broad-band photoexposure that encompassed the spectral band of the dye aggregate (~ 440 nm). In the presence of the donor compounds X-Y, the oxidized dye can be reduced according to Scheme 1. Photographic dispersions prepared without the addition of a spectral sensitizing dye were irradiated at 365 nm, which is within the band gap absorption of the silver halide.⁴ The product of excitation in this region is a conduction band electron and a hole in the valence band.⁴ In this case, injection of an electron into the valence band by X-Y (i.e., oxidation of X-Y by the hole in the valence band) can occur to initiate X-Y chemistry in a manner analogous to the dye-sensitized systems.

Any interaction of the electron donors with either the oxidized sensitizing dyes or the valence band holes presumably requires some degree of association of the molecules with the silver iodobromide grain surface. Because the X-Y molecules studied here contain no specific functional groups to promote chemisorptive binding to the silver halide, relatively high concentrations of the compounds were added to the dispersions to effect at least a small, equilibrium amount of associated, or physisorbed, compound. The practical upper limit on the concentrations of the X-Y compounds was largely determined by their overall solubility in the aqueous AgBr dispersion from which the photographic films were cast.

As described in more detail in the Experimental Section, the photosensitivity of the films was evaluated by measuring the exposure necessary to produce a specific optical density (0.2 above that of the unexposed films) after chemical development (reduction) using a hydroquinone-based developing solution. The

(38) Altman, J. H. In *The Theory of the Photographic Process*, 4th ed.; James, T. H., Ed.; MacMillan: New York, 1977; p 481.

(39) Farid, S. Y.; Lenhard, J. R.; Chen, C. H.; Muentner, A. A.; Gould, I. R.; Godleski, S. A.; Zielinski, P. A. U.S. Patent 5,747,235, 1998.

Table 2^a

Compound	($E^{\text{ox}}_{\text{X}^{\bullet}}$) ^a (V vs SCE)	Concentration ^b (10^{-3} mole/mole silver iodobromide)	Undyed ^c S_{365}	Blue-Dyed ^d S_{blue}
None			(1.00)	(1.00)
1	-0.86 ± 0.03	44	1.59	1.32
2	-0.96 ± 0.03	44	1.82	1.48
3	> -0.4	4.4	1.18	1.32
4	-0.56 ± 0.08	4.4	1.26	1.32
5	-0.79 ± 0.08	4.4	1.41	1.66
6	< -0.9	4.4	1.70	1.91
7	> -0.4	0.44	1.15	1.12
8	< -0.9	0.44	1.82	1.78
9	< -0.9	0.44	1.72	1.77
10	< -0.9	44	1.41	1.35

^a Estimated oxidation potential of the corresponding radical formed upon oxidative decarboxylation, in V vs SCE, from Table 1. ^b Concentration of added compound (1–10) relative to the concentration of silver iodobromide. ^c Sensitivity of undyed photographic films in the presence of added compound 1–10 relative to that in the absence of a fragmentable donor. ^d Sensitivity of blue-sensitized photographic films in the presence of added compound 1–10 relative to that in the absence of a fragmentable donor.

sensitivities of the undyed dispersion, S_{365} , and of that sensitized with the blue-absorbing dye, S_{blue} , are normalized relative to the corresponding film coatings containing no X–Y compound, Table 2.³⁹

The optimum concentration for each X–Y compound was found to be a function of its solubility, adsorptivity to silver halide, and the tendency toward dark (redox) reactions with silver iodobromide.⁴⁰ The data in Table 2 are those at the optimum concentration of each donor compound obtained over the range of concentrations examined. The differences in solubility and apparent adsorptivity, however, complicate the comparison of sensitivity results between the different kinds of X–Y molecule.

As the data of Table 2 indicate, each of the compounds 1–10 increases the photosensitivity of silver halide. The sensitivity increases observed on the blue-sensitized silver halide dispersion are fairly similar to those obtained on the undyed dispersion. This result may be expected, given that the potential energy of the oxidized blue-absorbing dye and that of the valence band are similar and are considerably more positive than the estimated values for ($E^{\text{ox}}_{\text{X–Y}}$). When data obtained within a given class of X–Y donors are compared, it is clear that those compounds that generate radicals with the most negative value of ($E^{\text{ox}}_{\text{X}^{\bullet}}$) yield the largest increases in photosensitivity. For example, the *N*-methylindole acetic acid compounds 3 and 4, which have ($E^{\text{ox}}_{\text{X}^{\bullet}}$) values that are significantly below the potential of the silver halide conduction band, increase the silver halide photosensitivity by about 20–30%. These results are consistent with a hole-trapping/X–Y fragmentation sequence that effectively competes with unwanted recombination reactions. With compound 5, the increase in photographic response is nearly twice as large (~40–60%). This compound has an ($E^{\text{ox}}_{\text{X}^{\bullet}}$) which

(40) A slight increase in the density of the unexposed region is noted for the silver iodobromide dispersion containing 7. This is probably associated with a redox (silver iodobromide reduction) reaction.

approaches that of the conduction band. Within this series of fragmentable donors, the highest increase in sensitivity (70 to 90%) is achieved with compound 6, which produces a highly reducing X^{\bullet} radical that is capable of injecting a second electron into the conduction band.

Similarly, a dramatic difference in activity is also observed for the dimethylaminophenylacetic acid derivatives, 7–9. Compound 7 yields a modest (12–15%) increase in silver halide sensitivity, consistent with its ability to fragment upon trapping the photohole without yielding a strongly reducing radical. Approximately 80% increase in sensitivity is obtained, however, with compounds 8 and 9, which upon fragmentation produce sufficiently reducing radicals to inject an electron into the conduction band.

The increase in sensitivity effected by compound 10 is somewhat lower than expected, considering that it also yields a strongly reducing radical. The reason is not clear, but it may be the result of poorer adsorption to the silver halide surface or poor association with the sensitizing dye.

Overall, the results of Table 2 demonstrate that a modest increase in silver halide photosensitivity is achieved with all of the fragmentable electron donor compounds. More significant sensitivity increases are obtained with those X–Y compounds that fragment to give radicals capable of injecting an electron directly into the silver halide conduction band in the manner outlined in Scheme 1. Extensive data on photographic evaluation of these and other fragmentable donors are given elsewhere.^{39,41}

Summary and Conclusions

A novel two-electron sensitization scheme for silver halide photography is described that is based on a secondary electron transfer reaction from an appropriately designed donor molecule to the oxidized sensitizing dye. From model studies in solution, a series of electron-rich carboxylate compounds has been identified to have the appropriate redox and fragmentation properties. Photographic sensitivity experiments show that the photosensitivity of photographic materials can be increased by a factor of nearly 2 by the use of the secondary donors. The close relationship between the behavior of the donor molecules in solution and that in the photographic system supports the proposed two-electron sensitization scheme.

Experimental Section

Materials. The synthesis of the X–Y compounds, 1–10, will be described elsewhere. The model compounds, 11–14, were commercially available (Aldrich) and were freshly distilled prior to use. The sensitizing dye, 15, was prepared according to general procedures for cyanine dye syntheses⁴² and is also commercially available from H.W. Sands Corp. 9,10-Dicyanoanthracene, DCA, (Kodak) was recrystallized twice from pyridine.³⁰ 2,9,10-Tricyanoanthracene⁴³ was prepared from the corresponding tribromoanthracene and was recrystallized from acetonitrile. 2,6,9,10-Tetracyanoanthracene, TCA, was available from earlier studies.^{30,44} Biphenyl (Aldrich) was recrystallized from ethanol. Acetonitrile (Baker, HPLC grade) was dried over 4 Å molecular sieves for electrochemical use. Tetrabutylammonium tetrafluoroborate was recrystallized from ethanol/water mixture.

(41) (a) Farid, S. Y.; Lenhard J. R.; Chen C. H.; Muentner A. A.; Gould I. R.; Godleski S. A.; Zielinski P. A.; Weidner, C. H. U.S. Patent 5,747,236, 1998. (b) Farid, S. Y.; Lenhard J. R.; Chen C. H.; Muentner A. A.; Gould I. R.; Godleski S. A.; Zielinski P. A.; Weidner, C. H. U.S. Patent 5,994,051, 1999.

(42) Hamer, F. M. In *The Chemistry of Heterocyclic Compounds*; Weissberger, A., Ed.; Interscience: New York, 1964; Vol. 18.

(43) Kikuchi, K.; Takahashi, Y.; Koike, K.; Wakamatsu, K.; Ikeda, H.; Miyashi, T. *Z. Phys. Chem. (Munich)* **1990**, 167, 27.

(44) Mattes, S. L.; Farid, S. *J. Am. Chem. Soc.* **1982**, 104, 1454.

Transient Absorption Experiments. The transient absorption experiments were carried out using a nanosecond excimer (Questek model 2000) pumped dye laser (Lambda Physik model FL 3002) as the excitation source ($\sim 1\text{--}2$ mJ, ~ 15 ns, 410 nm, DPS laser dye (Exciton)). The analyzing part of the experiment was of standard design, and used an Osram XBO 150W1 xenon arc lamp in an Oriel model 66060 housing, a PRA model 302 power supply, and a PRA model M-305 pulser, which increased the analyzing light intensity for ~ 2 ms. An ISA model H-20 monochromator and a Hamamatsu model 446 photomultiplier tube (PMT) were used. The output of the PMT was captured using a Tektronix model DSA 602 digital oscilloscope. The experiment was controlled using an IBM-compatible PC. Experiments were performed in 1 cm^2 cuvettes. The solutions were bubbled with argon or oxygen during the experiments which also served the purpose of mixing the solutions between laser shots. The absorbance of the sensitizer was typically ~ 0.8 at the excitation wavelength.

Electrochemistry. Redox potentials were measured by cyclic or AC voltammetry using a Princeton Applied Research Corp. (PAR) 173 potentiostat in conjunction with PAR models 175 universal programmer and a PAR 179 digital coulometer. Solutions for voltammetric examination contained acetonitrile, 0.1 M tetrabutylammonium fluoroborate, and $\sim 5 \times 10^{-4}$ M of the analyte. All solutions were deaerated with argon prior to examination. The working electrode was a Pt disk ($\sim 0.02\text{ cm}^2$) that was polished with $0.1\ \mu$ diamond paste (Buhler Metadi), and rinsed with water before each experiment. All potentials were measured versus the NaCl saturated calomel electrode at $22\text{ }^\circ\text{C}$.

Photographic Measurements. Silver iodobromide tabular silver halide dispersions were prepared by double-jet addition of aqueous AgNO_3 and sodium halide solutions to an aqueous gelatin solution. The silver ion activity was controlled to produce crystals of tabular morphology.^{39,45} The dispersion grains had an average thickness of $0.123\ \mu$ and an average circular diameter of $1.23\ \mu$. The dispersion was "chemically sensitized" by adding 1.2×10^{-5} mol/Ag mol of (1,3-dicarboxymethyl-1,3-dimethyl-2-thiourea) at $40\text{ }^\circ\text{C}$, the temperature was then raised to $60\text{ }^\circ\text{C}$ at a rate of $5\text{ }^\circ\text{C}/3$ min and the dispersion held for 20 min before cooling to $40\text{ }^\circ\text{C}$. 2,5-Disulfocatechol was subsequently added at a level of 1.3×10^{-2} mol/Ag mol to minimize the amount of

inadvertent latent image formation in unexposed silver halide grains. Portions of the silver halide dispersion were dyed by adding a methanolic solution of the sensitizing dye 5,5'-dichloro-*N,N'*-di-3-sulfopropylthiacyanine triethylammonium salt, **15**. The dye was added at $40\text{ }^\circ\text{C}$ to give a concentration of 0.9×10^{-3} mol dye/mol silver iodobromide, a quantity corresponding to approximately 90% of the amount required to form a complete monolayer on the crystal surfaces. Fragmentable electron donors, X-Y, were added from an aqueous potassium bromide solution, followed by additional water, gelatin, and surfactant to give a final dispersion melt that contained 216 g of gelatin per mol of silver. These silver halide dispersion melts were coated onto an acetate film base at 1.61 g/m^2 of Ag with gelatin at 3.22 g/m^2 . The films were protected with an overcoat containing gelatin at 1.08 g/m^2 , coating surfactants, and bisvinyl sulfonyl methyl ether as a gelatin-hardening agent.

Photographic sensitivity in the region of intrinsic silver halide light absorption was determined by exposing the coated samples for 0.1 s to a 365 nm line from a high pressure Hg lamp filtered through a Kodak Wratten filter number 18A. The samples were exposed through a neutral density filter providing a stepped series of optical densities ranging from 0 to 4 in 0.2 optical density steps. To determine the response in the spectral region where the sensitizing dye absorbs, coating samples were exposed for 0.1 s to a tungsten lamp filtered through a Kodak Wratten filter number 2B. This cutoff filter passes only light of wavelengths longer than 400 nm that is absorbed mainly by the sensitizing dye. These samples were exposed through a neutral density filter providing a stepped series of optical densities ranging from 0 to 3, in 0.2 increments. All exposed films were chemically developed for 6 min using a hydroquinone-containing Kodak Rapid X-ray Developer, fixed to remove undeveloped silver halide, and washed. The relative sensitivity at 365 nm, S_{365} , and at $\lambda > 400$ nm (absorbed by the blue-absorbing sensitizer), S_{blue} , were evaluated as the reciprocal exposure required to yield a density of 0.2 above the density of the unexposed region of the film. For each exposure the relative sensitivity was set equal to unity for the control coating with no added X-Y donors.

(45) Chang, E.; Friday, J. U.S. Patent 5,314,793, 1994.